ISSN 0021-3640, JETP Letters, 2007, Vol. 85, No. 12, pp. 658–661. © Pleiades Publishing, Ltd., 2007.
Original Russian Text © S.G. Barsov, S.I. Vorob'ev, V.P. Koptev, E.N. Komarov, S.A. Kotov, S.M. Mikirtych'yants, G.V. Shcherbakov, A.E. Pestun, Ya.M. Mukovskiĭ, 2007, published in Pis'ma v Zhurnal Éksperimental'noĭ i Teoreticheskoĭ Fiziki, 2007, Vol. 85, No. 12, pp. 795–798.

Muon Investigation of $HoMnO_3$ and $YMnO_3$ Hexagonal Manganites

S. G. Barsov[a], S. I. Vorob'ev[a, *], V. P. Koptev[a], E. N. Komarov[a], S. A. Kotov[a], S. M. Mikirtych'yants[a], G. V. Shcherbakov[a], A. E. Pestun[b], and Ya. M. Mukovskiĭ[b]

[a] *Petersburg Nuclear Physics Institute, Russian Academy of Sciences, Gatchina, Leningradskaya region, 188300 Russia*

**e-mail: vsiloa@pnpi.spb.ru*

[b] *Moscow State Institute of Steel and Alloys, Leninskiĭ pr. 4, Moscow, 119049 Russia*

Received May 21, 2007

The magnetic properties of multiferroics $HoMnO_3$ and $YMnO_3$ have been investigated using the muon (μSR) method. Analysis of the dependence of the dynamical relaxation rate λ and characteristics of the distribution of local static fields makes it possible to more precisely determine the phase states of the samples under investigation.

PACS numbers: 75.20.Hr, 75.30.Et, 75.47.Np, 75.50.Gg, 76.75.+i

DOI: 10.1134/S0021364007120156

During the past several years, interest in multiferroics, substances with coexisting magnetic and electric orderings, has increased sharply [1–3]. On the one hand, the creation of devices transforming information in the form of magnetization into an electric voltage and vice versa on a unified material platform is an attractive solution to urgent problems of sensor engineering, magnetic memory, and microelectronics, including spintronics, combining the advantages of power-independent magnetic memory and high-speed electric systems for information processing. On the other hand, owing to the experience accumulated since the discovery of the first multiferroics (beginning of the 1960s), substances with strong magnetoelectric properties can be created under usual conditions. For these reasons, the magnetoelectric subject is undergoing a renaissance, which is manifested in the appearance of sections devoted to multiferroics at symposiums on magnetism, in the appearance of special conferences, and in the exponential increase in the number of publications on this subject.

Manganites $RMnO_3$ exhibit a wide variety of physical properties, depending on the rare-earth element R. Compounds with a large ion radius of the element R (La, Pr, Nd, Sm, Eu, Gd, and Tb) are crystallized in the orthorhombic structure with the space group *Pnma* [4]. Compounds with a smaller ion radius of the element R (Ho, Er, Tm, Yb, Lu, Y, Sc, and In) exhibit the hexagonal crystal structure with the space group $P6_3cm$ [5]. The hexagonal manganites belong to ferroelectromagnetic materials in which the transition temperature to the ferroelectric state, $T_C \sim 600$–1000 K, is much higher than the temperature of antiferromagnetic ordering, $T_N \sim 70$–130 K [6].

This work is devoted to the investigation of local magnetic fields and their distribution in multiferroics $HoMnO_3$ and $YMnO_3$ by the muon method of substance investigation (μSR method). The samples were obtained by the solid-phase synthesis method. The measurements were performed on the muon channel of the synchrocyclotron at the Petersburg Nuclear Physics Institute, Russian Academy of Sciences, using a μSR setup [7].

The time distributions of the positrons, $N_e(t)$, which are formed in the decay of the μ^+ meson ($\mu^+ \longrightarrow e^+ + \nu_e + \tilde{\nu}_\mu$) and are emitted in the direction of the initial muon polarization in the time window $\Delta t \sim 4.5\tau_\mu$ after the stop of each muon in a sample, where τ_μ is the muon lifetime, were measured in the experiment. The time distribution of the positrons is described by the expression

$$N_e(t) = [N_0 \exp(-t/\tau_\mu)] \times [1 + a_s G_s(t) + a_b G_b(t)] + \Phi, \quad (1)$$

where N_0 is the normalization constant or, in other words, the number of detected positrons; $\tau_\mu \approx 2.19711 \times 10^{-6}$ s is the muon lifetime; a_s is the initial asymmetry of the muon decay stopped in the sample; a_b is the background component of a_s from muons stopped in the input windows of the cryostat and the master counter of the muon detector; $G_s(t)$ and $G_b(t)$ are the polarization relaxation function for the muons stopped

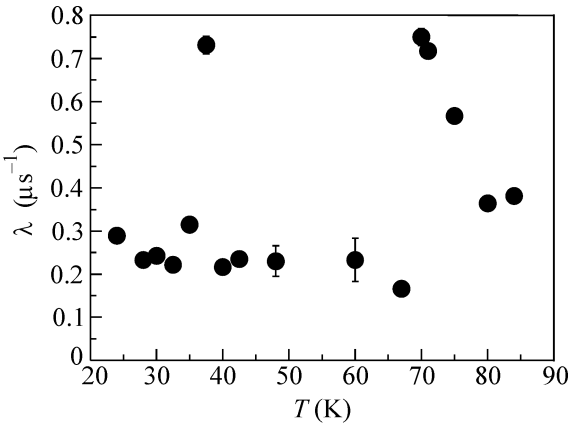

Fig. 1. Relaxation rate of the polarization of muons stopped in the $HoMnO_3$ sample in zero magnetic field.

in the sample and background sources, respectively; and Φ is the random coincidence background.

The experimental data are analyzed under the assumption of the factorization of the relaxation function:

$$G_s(t) = G_d(t)G_{st}(t), \quad (2)$$

where $G_d(t)$ describes the relaxation caused by the dynamical effects and $G_{st}(t)$ is the relaxation function in static fields. When studying the dynamical phenomena determining the muon spin relaxation, the relaxation function is specified as

$$G_d(t) = \exp(-\lambda t), \quad (3)$$

where λ is the dynamical relaxation rate.

Figure 1 shows the temperature dependence of the relaxation rate λ of the polarization of muons stopped in the $HoMnO_3$ sample in zero magnetic field. This dependence exhibits two peaks at 76 and 40 K, which correspond to two phase transitions. The first transition at $T = 76$ K is a transition from the paramagnetic state to the antiferromagnetic ordering state. The second transition at $T = 40$ K is associated with the rotation of the spins of Mn by 90° (spin-relaxation transition). This conclusion is in good agreement with the results obtained by other methods [8, 9].

Detailed analysis of the muon polarization relaxation function G_s makes it possible to determine the parameters of the distribution of local magnetic fields at various temperatures of the samples under investigation. In particular, the relaxation function of the polarization of muons stopped in the $HoMnO_3$ sample, $G_s(t)$, in zero magnetic field is described by the expression

$$G_s(t) = [a_1(1/3 + 2/3\cos(\Omega_1 t)\exp(-\Delta_1 t)) + a_2(1/3 + 2/3\cos(\Omega_2 t)\exp(-\Delta_2 t))]\exp(-\lambda t), \quad (4)$$

where $a_1 + a_2 = a_s$ is the initial asymmetry of the decay of muons stopped in the sample, λ is the dynamical relaxation rate, $\Omega_{1,2} = 2\pi F_{1,2}$ are the cyclic frequencies (associated with the mean local field at the muon localization site), and $\Delta_{1,2}$ is the frequency spread associated with the spread of internal magnetic fields.

For example, Figs. 2 and 3 show the polarization relaxation functions $G_s(t)$ for the $HoMnO_3$ sample at two temperatures ($T = 50$ K between the first and second phase transitions and $T = 30$ K after the second, spin-rotation transition).

Figure 4 shows the temperature dependence of the frequencies of the muon spin precession for the

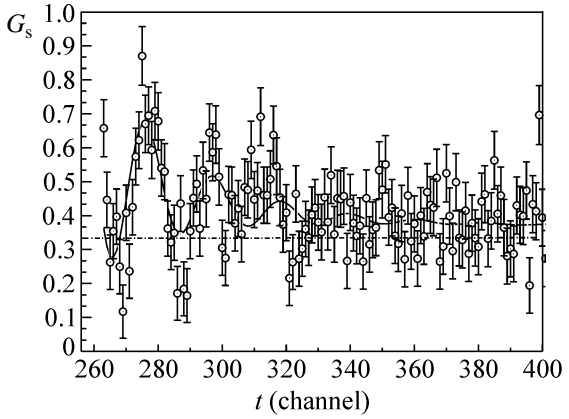

Fig. 2. Polarization relaxation functions $G_s(t)$ for the $HoMnO_3$ sample in zero magnetic field at a temperature of 50 K for the parameters $a_1 = 0.173(9)$, $a_2 = 0.099(9)$, $F_1 = 58(1)$ MHz, $\Delta_1 = 48(1)$ MHz, $F_2 = 0$, and $\Delta_2 = 37(7)$ MHz. One channel in the horizontal (time) scale corresponds to 0.8 ns, and the 256th channel corresponds to zero time.

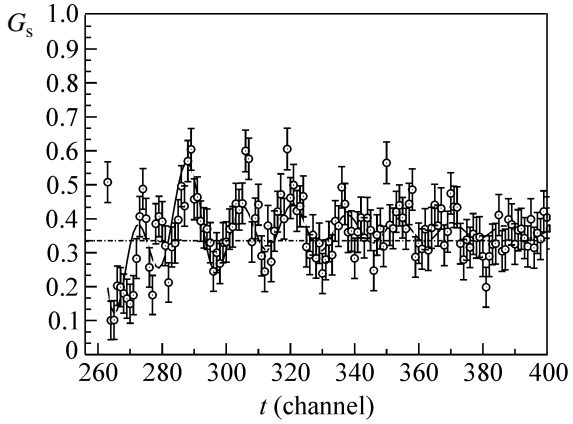

Fig. 3. Polarization relaxation functions $G_s(t)$ for the $HoMnO_3$ sample in zero magnetic field at a temperature of 30 K for the parameters $a_1 = 0.100(26)$, $a_2 = 0.172(26)$, $F_1 = 75(4)$ MHz, $\Delta_1 = 24(2)$ MHz, $F_2 = 40(1)$ MHz, and $\Delta_2 = 63(6)$ MHz. One channel in the horizontal (time) scale corresponds to 0.8 ns and the 256th channel corresponds to zero time.

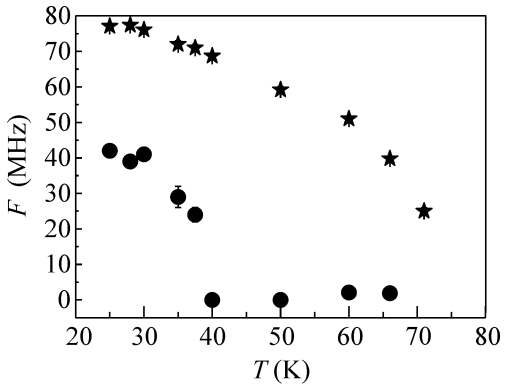

Fig. 4. Temperature dependence of the frequencies (stars) F_1 and (circles) F_2 of the precession observed for the $HoMnO_3$ sample in zero field.

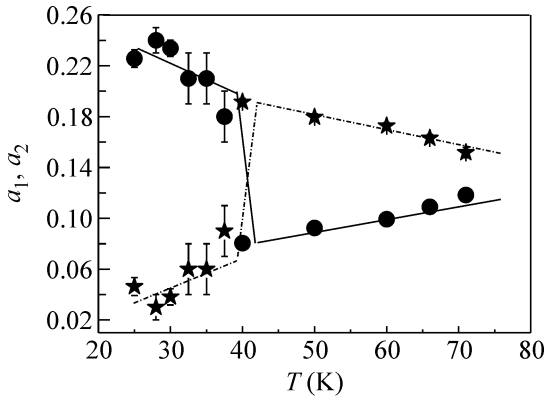

Fig. 5. Temperature dependence of the asymmetry coefficients (stars) a_1 and (circles) a_2, where $a_1 + a_2 = a_s$, for the $HoMnO_3$ sample in zero field. The lines are drawn to guide the eye.

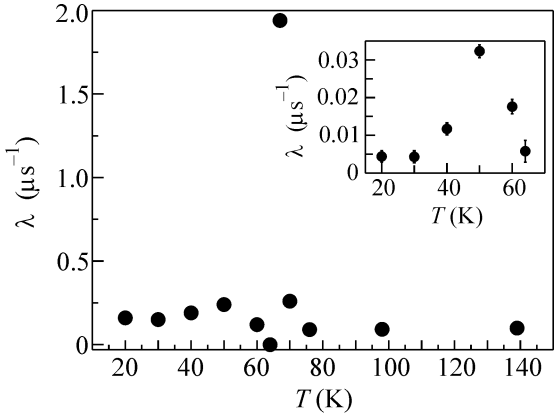

Fig. 6. Temperature dependence of the polarization relaxation rate for muons stopped in the $YMnO_3$ sample in zero magnetic field.

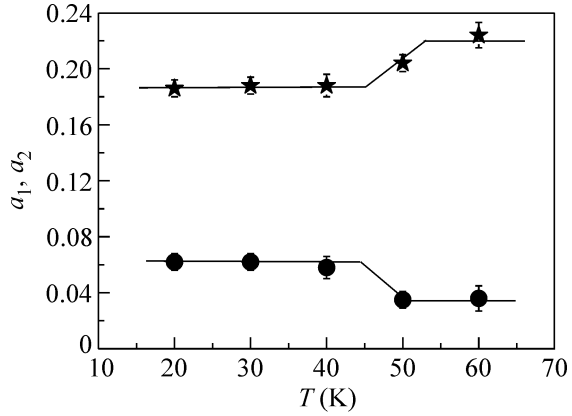

Fig. 7. Temperature dependence of the asymmetry coefficients (stars) a_1 and (circles) a_2, where $a_1 + a_2 = a_s$ for the $YMnO_3$ sample in zero field. The lines are drawn to guide the eye.

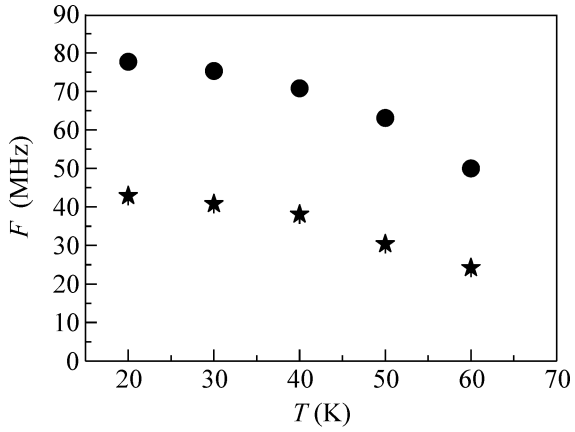

Fig. 8. Temperature dependence of the frequencies (stars) F_1 and (circles) F_2 of the precession observed for the $YMnO_3$ sample in zero field.

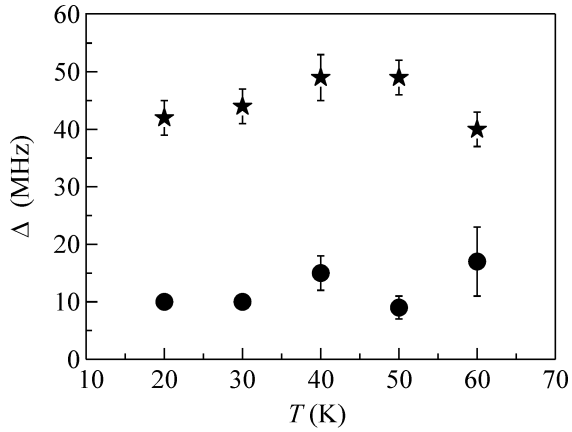

Fig. 9. Temperature dependence of the parameters (stars) Δ_1 and (circles) Δ_2 for the $YMnO_3$ sample.

$HoMnO_3$ sample in zero external magnetic field. It is seen that precession at two frequencies, one of which is negligibly low as compared to the other frequency ($F_1 \approx 40$ MHz and $F_2 \leq 1$ MHz), is observed for sample temperatures below $T = 76$ K. As the sample temperature is decreased, F_1 increases monotonically, whereas F_2 decreases. For sample temperatures below the temperature $T_{SR} \approx 42$ K, the frequency F_2 increases noticeably (almost from zero) and continues to monotonically increase with decreasing the temperature.

Figure 5 shows the temperature dependence of the coefficients a_1 and a_2 [see Eq. (4)]. It is seen that the relation between the coefficients a_1 and a_2 changes sharply at the temperature of the spin-rotation transition, $T_{SR} \approx 42$ K.

Similar investigations were performed for the $YMnO_3$ sample. Figures 6–9 show the results of the processing of the experimental data obtained with the $YMnO_3$ samples. The temperature dependence of the polarization relaxation rate λ for muons stopped in the $YMnO_3$ sample exhibits a peak at a temperature of $T =$ 66 K, which corresponds to the paramagnetic–antiferromagnetic phase transition (see Fig. 6). A nonmonotonic temperature behavior of the parameter λ is seen in the temperature interval of 45–55 K (see the inset in Fig. 6). Precession at two frequencies F_1 and F_2 is seen in the temperature interval of 20–60 K; the relation between the frequencies, $F_2/F_1 \approx 2$, holds in the indicated temperature interval (Fig. 8).

Figure 9 shows the temperature dependence of the parameters Δ_1 and Δ_2 (frequency spread) in the temperature interval of 20–60 K. Similar results were obtained in [10].

Note a feature in the behavior of the partial amplitudes a_1 and a_2 [see Eq. (4)] in the temperature interval of 20–60 K. A change in the ratio of these parameters, a_1/a_2, is observed at a temperature of $T \approx 50$ K (see Fig. 7).

Thus, the temperature dependences of the relaxation rate of the muon spin (shown in Fig. 6) and partial amplitudes a_1 and a_2 (shown in Fig. 7) for the $YMnO_3$ sample exhibit features at a temperature of ~50 K. This is likely attributed to the partial rotation of the manganese spins in the $YMnO_3$ compound [11].

The temperature dependence of the precession frequency for the $HoMnO_3$ and $YMnO_3$ samples is well approximated by the Curie–Weiss curve, $F \sim F_{max}(1 - T/T_N)^{\beta}$ with the exponent $\beta = 0.39 \pm 0.02$, which corresponds to the Heisenberg 3D magnet model.

We are grateful to R.V. Pisarev (Ioffe Physicotechnical Institute, Russian Academy of Sciences, St. Petersburg) for the samples placed at our disposal and for valuable stimulating discussions.

REFERENCES

1. A. K. Zvezdin and A. P. Pyatakov, Usp. Fiz. Nauk **174**, 465 (2004) [Phys. Usp. **47**, 416 (2004)].
2. M. Fiebig, J. Phys. D: Appl. Phys. **38**, 123 (2005).
3. W. Prellier, M. P. Singh, and P. Murugavel, J. Phys.: Condens. Matter **17**, 803 (2005).
4. M. A. Gilleo, Acta Crystallogr. **10**, 161 (1957).
5. M. Fiebig, D. Fr¨phlich, K. Kohn, et al., Phys. Rev. Lett. **84**, 5620 (2000).
6. T. Katsufuji, M. Masaki, A. Machida, et al., Phys. Rev. B **66**, 134434 (2002).
7. S. G. Barsov, S. I. Vorob'ev, V. P. Koptev, et al., Preprint No. 2694, PIYaF RAN (Petersburg Inst. of Nuclear Physics, Russian Academy of Sciences, Gatchina, 2006).
8. B. Lorenz, A. P. Litvinchuk, M. M. Gospodinov, and C. W. Chu, Phys. Rev. Lett. **92**, 087204 (2004).
9. B. Lorenz, Y. Q. Wang, Y. Y. Sun, and C. W. Chu, Phys. Rev. B **70**, 212412 (2004).
10. T. Lancaster, S. J. Blundell, D. Andreica, et al., Phys. Rev. Lett. **98**, 197203 (2007).
11. P. J. Brown and T. Chatterji, J. Phys.: Condens. Matter **18**, 10085 (2006).

Translated by R. Tyapaev